

# Kinetic study of calcite particle (powder) thermal decomposition: Part I

A. Escardino\*, J. Garcia-Ten, C. Feliu

*Instituto de Tecnología Cerámica, Asociación de Investigación de las Industrias Cerámicas, Universitat Jaume I, Castellón, Spain*

Received 9 June 2007; received in revised form 22 January 2008; accepted 17 May 2008

Available online 30 June 2008

## Abstract

In the first step of the firing cycle used to manufacture white-firing wall tile bodies, the calcium carbonate that is added, as a source of CaO, to the clay raw materials mixture used to form these bodies needs to decompose. In order to study the kinetics of this process, a representative rate equation of the chemical reaction step of calcium carbonate thermal decomposition is needed.

There is a disparity of opinions regarding the reaction order of this chemical reaction step. For this reason, it was decided to obtain a rate equation for this chemical decomposition step, using the same type and size calcite particles that are usually added to these clay mixtures in industrial practice.

The present paper proposes a rate equation for this chemical reaction step. With this rate equation and the application of the “Uniform Conversion Model”, an expression has been derived that relates the fractional calcium carbonate conversion, in the studied calcite particles, to residence time and operating temperature. The equation satisfactorily fits the experimental results obtained under isothermal conditions in the studied temperature range for particles smaller than 100  $\mu\text{m}$ .

The calcite particles studied are highly porous aggregates (smaller than 1.1 mm) of very small single crystals (smaller than 20  $\mu\text{m}$ ). The experiments were conducted in the 850–950 °C temperature range.

© 2008 Elsevier Ltd. All rights reserved.

*Keywords:* Calcination; Powders-gas phase reaction

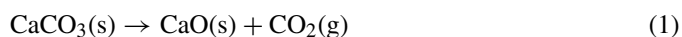
## 1. Introduction

Ceramic wall tile bodies have high porosity, low moisture expansion, and high dimensional stability as a result of the formation of certain crystalline phases in the firing stage, usually involving calcium silicates and aluminosilicates (gehlenite, anorthite, and wollastonite). These crystalline phases form at temperatures above 870 °C as a result of the reaction of CaO with  $\text{Al}_2\text{O}_3$  and  $\text{SiO}_2$  stemming from the decomposition of the clay minerals present in the starting raw materials mixture.<sup>1–3</sup>

The raw materials mixture used to make wall tile bodies typically contains 10–15% (by weight) calcium carbonate, which on decomposing during firing contributes the calcium oxide required to produce the foregoing crystalline phases. The clays used in making red-firing bodies contain the necessary calcium carbonate; however, the clays used to fabricate white-firing bod-

ies usually contain no carbonates, so that an appropriate quantity of calcite particles (which are smaller than 100  $\mu\text{m}$ ) is added as a source of CaO, calcite being cheaper than other calcium-containing minerals, such as wollastonite.<sup>4,5</sup>

The calcite particles initially present in the raw materials mixture used to make white-firing bodies decompose above 600 °C during the firing stage, releasing carbon dioxide, according to the following reaction scheme<sup>6</sup>:



When these particles are sufficiently small and ceramic body permeability is sufficiently elevated, this reaction is usually completed before the glaze sealing temperature (temperature at which the molten glaze fully covers the body) is reached. If the firing cycle (temperature–time) is not suitably designed, however, decomposition may still be ongoing when the glaze sealing temperature is reached. When this occurs, the carbon dioxide that is still being liberated in the body may be trapped in the molten glaze as small bubbles. Depending on glaze melt viscosity, these bubbles may reach the glaze outer surface and produce various defects, such as dimples, pinholing, or exces-

\* Corresponding author.

E-mail address: [aescardino@itc.uji.es](mailto:aescardino@itc.uji.es) (A. Escardino).

### Nomenclature

$c_B$	molar concentration of $\text{CaCO}_3$ in the particle after time $t$ has elapsed ( $\text{kmol}/\text{m}^3$ )
$c_B^0$	initial molar concentration of $\text{CaCO}_3$ in the particle ( $\text{kmol}/\text{m}^3$ )
$c_Q^G$	molar concentration of $\text{CO}_2$ in the gas phase ( $\text{kmol}/\text{m}^3$ )
$c_{QS}^G$	molar concentration of $\text{CO}_2$ next to the interface, gas side ( $\text{kmol}/\text{m}^3$ )
$c_{Qi}^S$	molar concentration of $\text{CO}_2$ at the reaction interface ( $\text{kmol}/\text{m}^3$ )
$c_{QS}^S$	molar concentration of $\text{CO}_2$ next to the interface, solid side ( $\text{kmol}/\text{m}^3$ )
$k$	rate constant of the direct reaction ( $\text{kmol}^{2/3}/(\text{m min})$ )
$k'$	rate constant of the reverse reaction ( $\text{m}/\text{min}$ )
$N_B$	moles of $\text{CaCO}_3$ after time $t$ has elapsed ( $\text{kmol}$ )
$N_B^0$	initial moles of $\text{CaCO}_3$ ( $\text{kmol}$ )
$r$	reaction or decomposition rate of $\text{CaCO}_3$ ( $\text{kmol}/(\text{m}^2 \text{min})$ )
$r_S$	initial radius of the $\text{CaCO}_3$ particle ( $\text{m}$ )
$R_B$	reaction rate in reference to $\text{CaCO}_3$ ( $\text{kmol}/\text{min}$ )
$S_e$	initial specific surface area of the $\text{CaCO}_3$ particle ( $\text{m}^2/\text{m}^3$ )
$S_i$	reaction interface area ( $\text{m}^2$ )
$S_{sp}$	specific surface area of the $\text{CaCO}_3$ particle ( $\text{m}^2/\text{g}$ )
$S_{PB}^0$	solid–gas interface area (particle surface) ( $\text{m}^2$ )
$t$	reaction time ( $\text{min}$ )
$T$	temperature ( $^\circ\text{C}$ )
$V_{PB}$	volume of the $\text{CaCO}_3$ particle after time $t$ has elapsed ( $\text{m}^3$ )
$V_{PB}^0$	initial volume of the $\text{CaCO}_3$ particle ( $\text{m}^3$ )
$W_Q^G$	$\text{CO}_2$ flow rate from the solid–gas interface to the gas phase ( $\text{kmol CO}_2/\text{min}$ )
$W_Q^S$	$\text{CO}_2$ flow rate from the reaction interface to the solid–gas interface ( $\text{kmol CO}_2/\text{min}$ )
$X$	$\text{CaCO}_3$ degree of conversion
<i>Greek letters</i>	
$\varepsilon$	porosity
$\rho_B$	apparent molar density of $\text{CaCO}_3$ in the particle after time $t$ has elapsed ( $\text{kmol}/\text{m}^3$ )
$\rho_B^0$	initial apparent molar density of $\text{CaCO}_3$ in the particle ( $\text{kmol}/\text{m}^3$ )
$\nu_B, \nu_Q, \nu_P$	stoichiometric coefficients of $\text{CaCO}_3, \text{CO}_2,$ and $\text{CaO}$

sive inner porosity of the end glaze. Fig. 1 presents an example of pinhole defects.

At present, the temperature range and time, during firing, that the calcite particles contained in the ceramic body are assumed to need in order fully to decompose are established empirically by manufacturers on the basis of industrial experience. No studies are available on the thermal decomposition, during

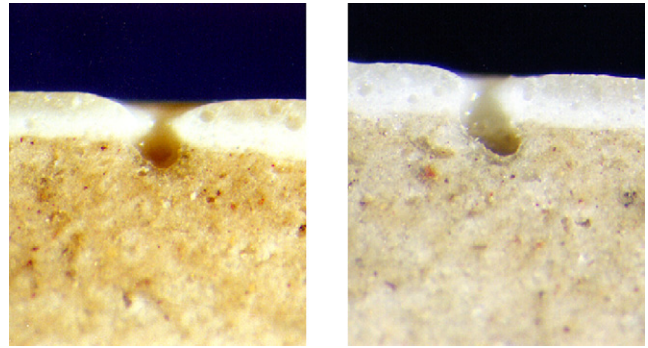


Fig. 1. Pinhole defects in wall tiles.

firing, of the calcium carbonate contained in green wall tile bodies; nor have any relevant scientific foundations been put forward. For this reason it was considered of interest to establish a mathematical expression that would relate the degree of advance of the decomposition process of the calcite particles, uniformly distributed throughout the initial mass of the body, to the main operating variables (time, temperature, body thickness and porosity, etc.), in order to be able to calculate, in each case, the most appropriate time range for complete calcite particle decomposition during firing.

In order to obtain this mathematical expression, after a feasible kinetic model is proposed, a representative equation of the overall process rate needs to be derived as an intermediate step.

To obtain the equation representing the overall process rate, it is essential first to have the rate equation for the chemical reaction step of  $\text{CaCO}_3$  decomposition in the calcite particles.

Although numerous studies have addressed the decomposition of calcium carbonate bodies (of different nature, size, and shape), there are discordant values for the apparent reaction order generally proposed for this reaction step, depending on the type and properties (size, shape, purity, and characteristics) of the sample and the experimental method and operating conditions used (Table 1) [7,8]. No clear trends are discernible in this regard in the literature.

Given this disparity of opinions, prior to studying the decomposition of the calcium carbonate initially contained in white-firing wall tile bodies during firing, it was decided to obtain a rate equation for the chemical decomposition step of the type and size of calcite particles that are usually added to these bodies. For this purpose, a study has been undertaken of several fractions of calcite particles similar to those used in industrial practice; the particles had different average sizes, which were always smaller than 1.1 mm.

## 2. Materials and experimental procedure

### 2.1. Materials

The study was conducted with natural calcite particles, supplied by REVERTE S.A., of the same nature and size range as those typically used in industrial practice to prepare the raw materials mixture for white-firing wall tile bodies. Their characteristics are described below.

Table 2 details the chemical composition of the calcite used.

Table 1  
Apparent activation energy values and reaction order proposed in the literature

Apparent activation energy (kJ/mol)	Apparent reaction order	Sample	Atmosphere	Reference	Year
159	1	Powder	Vacuum	Slonim	1930
397	1	Powder		Maskill, Turner	1932
155–163	0.3	Powder	Vacuum	Splichal, Skramovsky, Goll	1937
205	0–1	Powder	–	Kappel, Hüttig	1940
197	–	–	–	Bischoff	1950
147–176	0.58–0.72	Powder	Vacuum	Britton, Gregg, Winsor	1952
179	0.22	–	–	Kissinger	1957
163	0.4	–	–	Freeman, Carroll	1958
180	0.22	–	–	Barret, Perret, DeHartoulari	1959
170	0.67	Pellets and crystals	Air	Ingraham, Marier	1963
180–193	≈0.5	Pellet and powder	–	Sharp, Wentworth	1969
173	–	–	N <sub>2</sub>	Draper, Sveum	1970
172–210	0.2–0.53	Small blocks	N <sub>2</sub>	Auffredic, Vallet	1967, 1970
190–208	0.5	Powder	O <sub>2</sub>	Gallagher, Johnson	1973
205	1	Crystals	Vacuum	Beruto, Searcy	1974

Table 2  
Chemical composition (% by weight)

SiO <sub>2</sub>	0.2
Al <sub>2</sub> O <sub>3</sub>	0.1
Fe <sub>2</sub> O <sub>3</sub>	0.05
TiO <sub>2</sub>	–
Na <sub>2</sub> O	–
K <sub>2</sub> O	0.01
CaO	55.7
MgO	0.20
L.O.I.	43.5

The table shows that the impurities content is very low. The calcium content (55.7% by weight) is practically the same as in the pure calcium carbonate (56%). Several particle size fractions of this type of calcite were prepared by dry milling, in a ball mill, and screening in a sieve shaker with nested screens. The average particle diameter of each studied fraction was determined by screen analysis. The reference assigned to each particle size fraction and the average particle radius<sup>9</sup> are shown in Table 3. This table also presents the specific surface area measurements of the different test particle size fractions. It may be observed that this last characteristic is practically independent of average particle radius and has a mean value of 0.60 m<sup>2</sup>/g, if the instrumental error is taken into account. The specific surface area was determined by nitrogen adsorption at –196.15 °C (BET method) with a MICROMERITICS TRISTAR 3000 Gas Adsorption Analyser.

The apparent density, determined experimentally, of the calcite particles used was 2270 kg/m<sup>3</sup>, which is equivalent to 22.7 kmol of CaCO<sub>3</sub>/m<sup>3</sup>, and calcite particle porosity was 16.5%.

Table 3  
Average radius ( $r_s$ ) and specific surface area ( $S_{sp}$ ) of the different test particle size fractions

	Particle size fraction							
	A	B	C	D	E	F	G	H
$r_s$ (μm)	1050	700	460	300	225	120	81	62
$S_{sp}$ (m <sup>2</sup> /g)	0.61	0.59	0.55	0.57	0.60	0.64	0.61	0.57

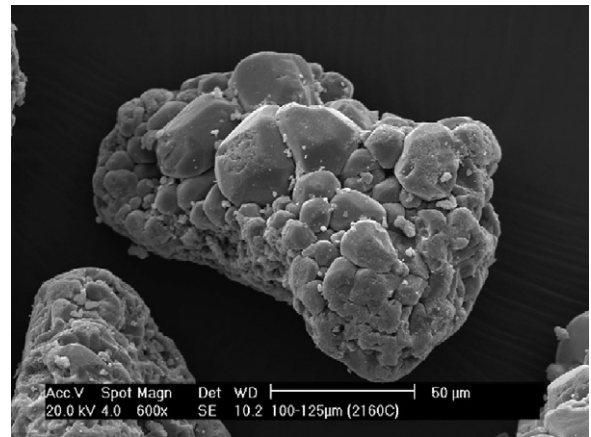


Fig. 2. Micrograph of one of the calcite particles.

Figs. 2 and 3 present the micrographs, obtained by scanning electron microscopy (PHILIPS Model XL30), of one of the calcite particles used. These particles, like the particle shown, consisted of crystalline aggregates of calcite microcrystals smaller than 20 μm and displayed an apparently highly porous structure, consistent with the porosity value ( $\epsilon = 0.165$ ) found.

## 2.2. Experimental assembly

The calcium carbonate decomposition reaction during firing was monitored by measuring sample weight loss during isothermal treatment in a laboratory tubular kiln. Air was fed into the kiln at a controlled temperature and speed. Fig. 4 schematically

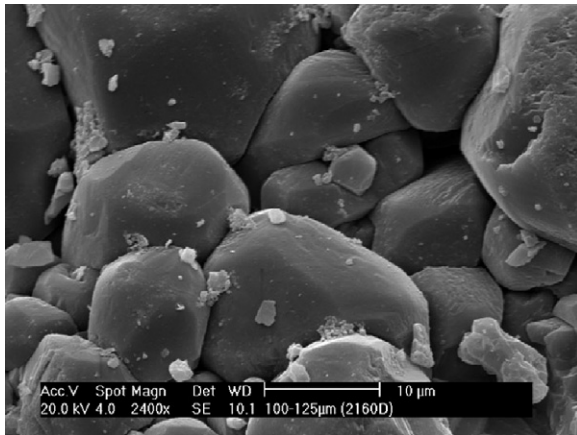


Fig. 3. Detail of the microcrystals making up the particle in Fig. 2.

illustrates the experimental assembly used. The assembly consisted of a refractory steel holder for the sample, located in the middle of the kiln-firing chamber. The holder was suspended from a single-pan balance by an alumina rod, so that sample mass could be continuously measured. The balance was connected to a computer with the appropriate software to record the pairs of mass–time values.

### 2.3. Experimental procedure

All experiments were carried out under isothermal conditions in air atmosphere, using a sufficiently high gas flow rate for the material (carbon dioxide) transfer step from the calcite particle interface to the gas phase not to affect the overall process rate.

The quantity of sample used in each experiment was  $500 \pm 10$  mg. This was uniformly spread in a thin layer of particles on a flat capsule. The sample had been previously weighed and heated to  $110^\circ\text{C}$  in a drying oven.

After calibration of the balance, the data logging system was switched on, and the capsule was quickly placed in the kiln. The pairs of mass–time values were recorded throughout each experiment, which ended when the variation in sample mass remained practically constant.

These measurements allowed calculation of the degree of conversion ( $X$ ), corresponding to the  $\text{CaCO}_3$  decomposition reaction with heat treatment. The fractional conversion degree

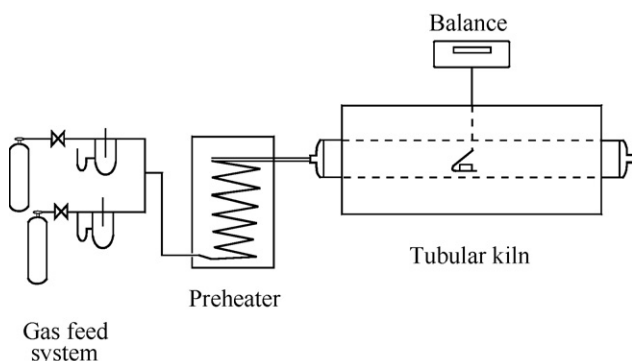


Fig. 4. Schematic illustration of the experimental set-up used.

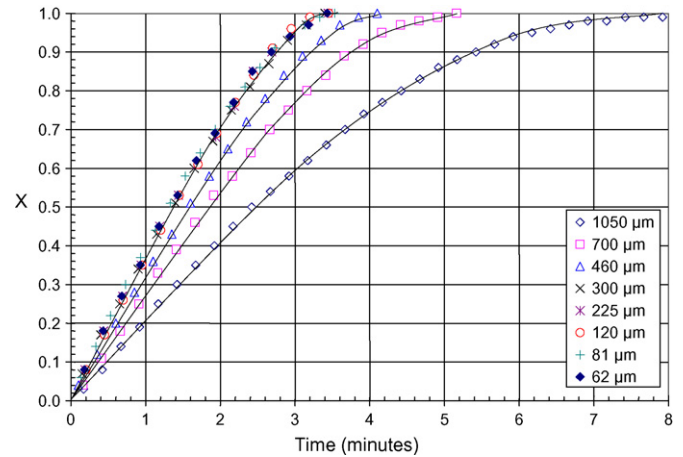


Fig. 5. Variation of calcium carbonate degree of conversion with time at  $850^\circ\text{C}$ .

was determined from the equation:

$$X = \frac{\Delta M}{\Delta M_\infty}$$

where  $\Delta M$  is mass loss of the sample at a given time ( $t$ ) after experiment commencement, and  $\Delta M_\infty$  is mass loss of the sample at a sufficiently long time to achieve constant weight, when all the calcium carbonate is assumed to have decomposed.

### 2.4. Experimental results

The results obtained in the form  $X$  (fractional conversion) versus  $t$  (residence time) at the five test temperatures ( $850$ ,  $875$ ,  $900$ ,  $925$ , and  $950^\circ\text{C}$ ) for the seven studied particle size fractions have been plotted in Figs. 5–9. In these figures the induction time, which ranged from 0.20 min for the highest temperature and smallest average particle radius to 0.35 min for the lowest temperature and largest average particle radius, has been subtracted from the experimentally measured time to allow the  $X=f(t)$  curves to pass through the origin of the coordinates ( $t=0$ ).

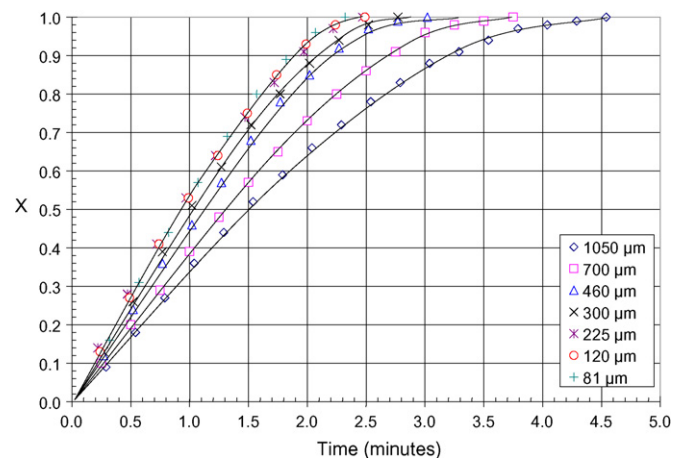


Fig. 6. Variation of calcium carbonate degree of conversion with time at  $875^\circ\text{C}$ .



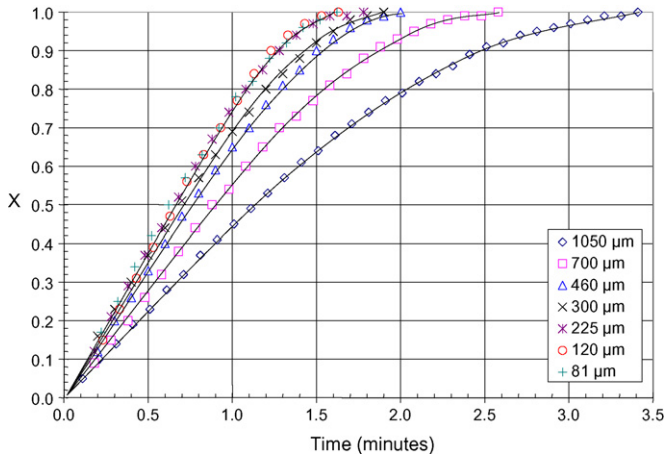


Fig. 7. Variation of calcium carbonate degree of conversion with time at 900 °C.

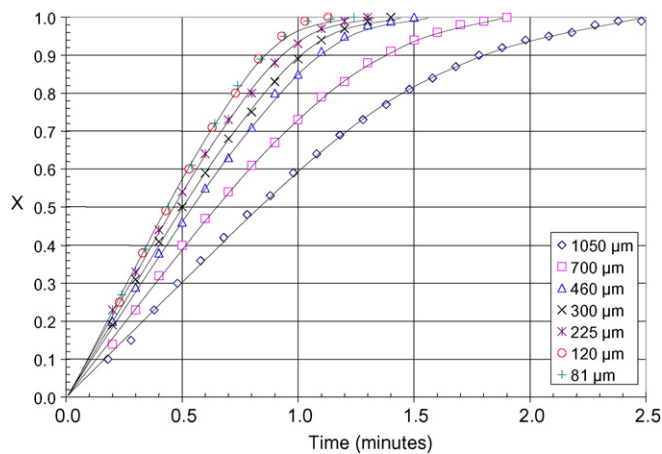


Fig. 8. Variation of calcium carbonate degree of conversion with time at 925 °C.

### 2.5. Discussion of results: proposed kinetic model

As Figs. 5–9 show, the experimental data of  $X$  versus residence time, corresponding to the particle size fractions with an average radius equal to or smaller than 300  $\mu\text{m}$  (at 850 °C), 225  $\mu\text{m}$  (at 875 and 900 °C), or 120  $\mu\text{m}$  (at 925 °C), practically coincide at each temperature, whereas those corresponding to

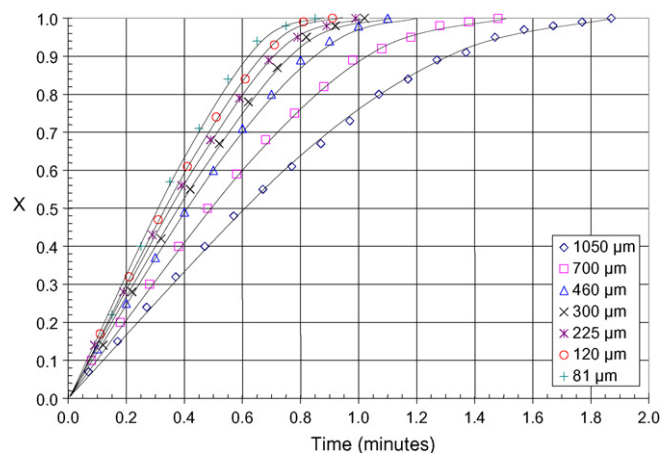


Fig. 9. Variation of calcium carbonate degree of conversion with time at 950 °C.

larger sizes fit different curves whose slope, for any value of  $t$ , decreases as average particle radius increases. Thus, in the calcite particle size fractions for which the results at the same temperature coincided, the overall decomposition process rate did not appear to be affected by the size of these particles. This was the case for the particle size fractions with an average radius equal to or smaller than 120  $\mu\text{m}$  at the lowest four test temperatures (850, 875, 900, and 925 °C).

Since the main objective of this study was to obtain a rate equation representing only the chemical reaction of calcium carbonate thermal decomposition, in the following, the discussion will only deal with the experimental results corresponding to the particle size fractions and temperatures for which the coinciding situation indicated in the foregoing paragraph occurs. The remaining curves will be dealt with in a subsequent paper.

Of all the kinetic models proposed in the literature for gas–solid systems, the only model in which overall process kinetics does not depend on the particle size of the reactant solid is the so-called *Homogeneous Reaction Model*<sup>10,11</sup> or *Uniform Conversion Model*<sup>12</sup> or *Uniform Reacting Pellets Model*<sup>13,14</sup> (depending on the author or researcher), when the chemical reaction step is assumed to be the overall process rate-limiting step. The term *Uniform Conversion Model (UCM)* will be used hereafter.

Since the calcite particles used are microcrystal aggregates (Fig. 2), each particle may be likened to a pellet made up of a group of grains, in this case, the microcrystals. Therefore, the model for gas–solid reactions that appears most suitable for interpreting the results is the “Grainy Pellet Model” (GPM),<sup>14–19</sup> illustrated in Figs. A.2 and A.3. The behaviour of the *GPM* coincides with that of the *UCM* when the chemical step unfolds much more slowly than that of diffusion of the gaseous component in each grain (intragrain diffusion) and between the grains (intergrain diffusion) making up the pellet.<sup>13,14,16–18</sup> When the grain size is very small, this assumption is more valid.<sup>16–18</sup>

Thus, in the case being considered, if the intergrain diffusion step (i.e. between the microcrystals making up the calcite particles) and the intragrain diffusion step (i.e. through each  $\text{CaCO}_3$  microcrystal) of the carbon dioxide that evolves as a result of the decomposition reaction unfold much more rapidly than the calcium carbonate chemical decomposition step in each microcrystal, one might assume that this last step is the overall process rate-controlling step. This would allow the *UCM* to be applied in order to derive an expression with which to attempt to correlate the experimental results obtained under the operating conditions in which the coincidence described above was observed.

For such a hypothesis to be viable, the calcite pellets (crystalline aggregates) and their grains need to be sufficiently small, and their structure and that of the  $\text{CaO}$  that forms during decomposition in each microcrystal (grain) need to be sufficiently porous for carbon dioxide diffusion through both structures to be much faster than the chemical decomposition reaction step.

The first condition seems to be met in this case, to judge by the appearance and size of the particles and grains (Fig. 2) and by their relatively high porosity. In order to evaluate compliance with the second condition, the appearance of the microcrystals making up the particles before and after heat treatment at 900 °C

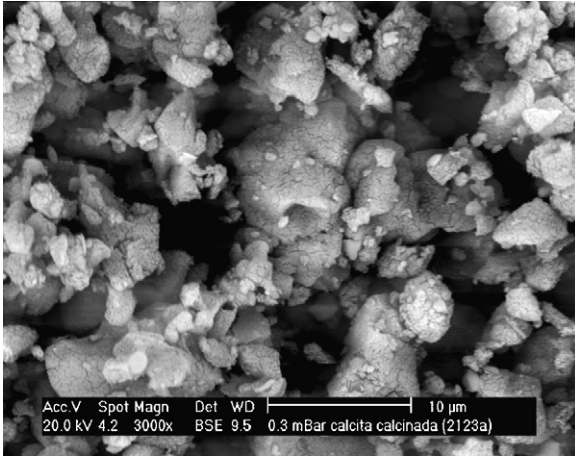


Fig. 10. Micrograph showing the appearance of the microcrystals in one of the calcite particles after heat treatment at 900 °C for 6 min.

for 6 min was observed by SEM. The micrograph in Fig. 10 clearly shows that the microcrystals are crazed and full of fissures after the heat treatment, facilitating CO<sub>2</sub> diffusion from calcium carbonate decomposition through the very porous CaO structure formed in each microcrystal.

Furthermore, for the UCM appropriately to represent the experimental results, the particle specific surface area needs to be independent of particle size in the range of values in which the coinciding results described above occurred. This circumstance is also practically met, as Table 3 shows.

In view of the foregoing results, the feasibility of using this kinetic model was tested, assuming that the CaCO<sub>3</sub> chemical decomposition step was process controlling, in order to try to derive an expression that would allow the experiment results to be correlated with the operating conditions under which the experiment results had been observed not to depend on particle size.

Operating in the form described in Appendix A, an expression has been derived of the form:

$$X = f(S_e, k, k', c_B, c_Q^G, t) \quad (2)$$

which is valid for a single calcite particle, assumed to be spherical. This expression relates  $X$ , which is the CaCO<sub>3</sub> degree of conversion in B (calcite particle considered), to particle residence time in the reactor ( $t$ ), under isothermal operating conditions; to the rate constants of the direct and reverse reactions ( $k$  and  $k'$ ), which depend on working temperature; to the specific surface area of the calcite particle ( $S_e$ ) and its molar concentration of CaCO<sub>3</sub> ( $c_B$ ); and to the molar concentration of carbon dioxide in the gas phase present in the system ( $c_Q^G$ ).

The rate equation of the calcium carbonate chemical decomposition step that led to the mathematical expression (2) that best fitted the experimental results was

$$r = kc_B^{1/3} - k'c_{Qi}^S = k[c_B^0(1 - X)]^{1/3} - k'c_{Qi}^S \quad (3)$$

where  $r$  is expressed in kmol/(min m<sup>2</sup>),  $k$  in kmol<sup>2/3</sup>/(m min), and  $k'$  in m/min. In this expression  $c_B$  and  $c_{Qi}^S$  represent, respectively, the molar concentration of calcium carbonate in the calcite par-

ticle considered and the molar concentration of carbon dioxide at the reaction interface. The reverse reaction was assumed, in principle, to be a first-order reaction in regard to the CO<sub>2</sub> concentration at the reaction interface, taking into account other researchers' views<sup>20</sup> and our own results.<sup>21</sup>

In this case it was not necessary to consider the term of the rate equation corresponding to the reverse reaction, since the operation was conducted using air free of carbon dioxide. However, in order to be able to study the thermal decomposition of the calcite particles contained in the ceramic bodies during firing, a representative rate equation of the chemical step of calcium carbonate thermal decomposition is needed, which contains the term corresponding to the reverse reaction, since this reaction is reversible and in the industrial kilns where white-body wall tiles are fired, the atmosphere in contact with the pieces contains about 5–8% CO<sub>2</sub> (by volume) because the heating is done using natural gas burners, with a direct flame.

Rate Eq. (3) has not been derived from any concrete kinetic model, but has been obtained by analogy, after trying other similar equations that did not fit the experimental data as well as this.

Expressing Eq. (3) in decomposed kmol of B (CaCO<sub>3</sub>) per unit time gives:

$$R_B = \nu_B S_e V_{pB}^0 [kc_B^{0/3} (1 - X)^{1/3} - k'c_{Qi}^S] \quad (4)$$

In this equation  $\nu_B = -1$  (see reaction scheme (1));  $S_e$  represents the specific surface area of the particle considered, expressed in m<sup>2</sup>/m<sup>3</sup> particle; and  $V_{pB}^0$  is the particle volume.

The rate equation (Eq. (4) and the corresponding mass balance in reference to the solid component B yielded the differential equation (deduced in Appendix A):

$$\frac{dX}{dt} = \frac{S_e}{c_B^0} [kc_B^{0/3} (1 - X)^{1/3} - k'c_Q^G] \quad (5)$$

where  $c_Q^G$  represents the molar concentration of carbon dioxide in the gas phase.

Analytical integration of this equation between indefinite limits, assuming carbon dioxide concentration in the gas phase to be  $c_Q^G = 0$  (as a result of using a CO<sub>2</sub>-free gas stream during the experiment), yielded the expression:

$$1 - (1 - X)^{2/3} = \frac{2}{3} S_e k c_B^{0-2/3} t \quad (6)$$

The procedure used to compare Eq. (6) with the results obtained in the series of experiments under consideration is described below.

Fig. 11 presents the experimental results obtained in the form  $F(X) = 1 - (1 - X)^{2/3}$  versus residence time ( $t$ ) for each test temperature. The experimental results fit a set of straight lines well, each of which corresponds to one of the test temperatures.

The value of the rate constant  $k$  in Eqs. (3)–(6) at each temperature was calculated from the slope of the corresponding straight line in Fig. 11, considering a mean value of  $S_e = 1.362 \times 10^6$  m<sup>2</sup>/m<sup>3</sup>, equivalent to 0.60 m<sup>2</sup>/g calcite particle, for all studied particle size fractions and a mean apparent mass density of 2270 kg/m<sup>3</sup> for each particle, equivalent to an initial

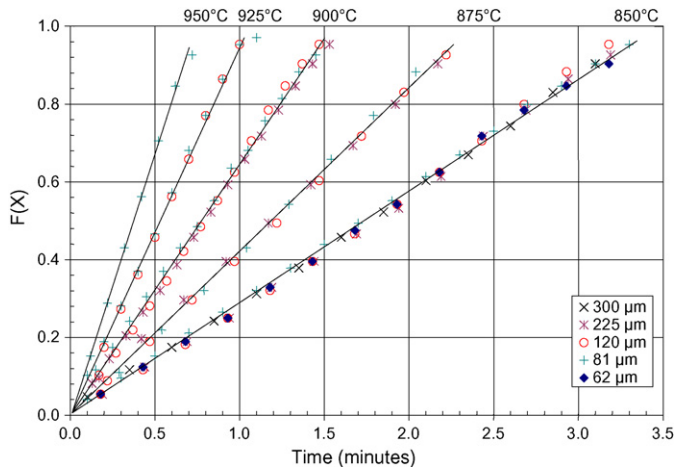


Fig. 11. Correlation of the experimental results by Eq. (6).

Table 4  
Values of *k* in Eq. (3)

<i>T</i> (°C)	<i>k</i> × 10 <sup>6</sup> (kmol <sup>2/3</sup> /(m min))
849.85	2.55
874.85	3.90
899.85	5.60
924.85	8.30
949.85	11.90

density or molar concentration (*c*<sub>B</sub><sup>0</sup>) of 22.7 kmol/m<sup>3</sup> (Section 2.1). The calculated values of the rate constant *k* are detailed in Table 4.

When the variation in the values of *k*, detailed in Table 4, was plotted against the inverse of temperature, expressed in degrees Kelvin, on semi-logarithmic coordinates (Fig. 12), a straight line was obtained from which the following equation was derived:

$$k = 367 \exp\left(-\frac{175384}{RT}\right) \quad (7)$$

where *R* = 8.3140 J mol<sup>-1</sup> K<sup>-1</sup>.

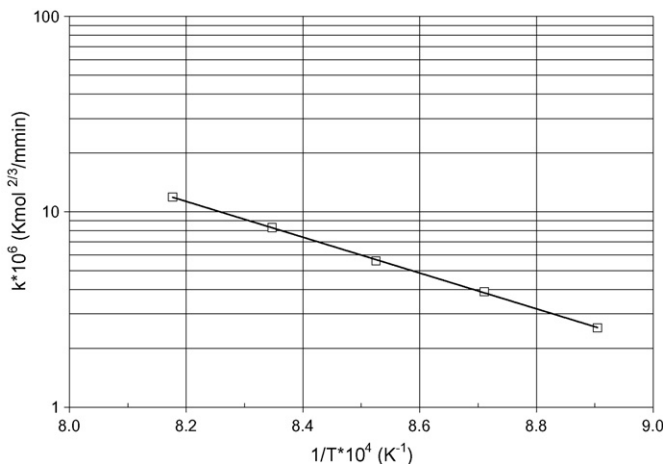


Fig. 12. Variation of *k* with the inverse of reaction temperature.

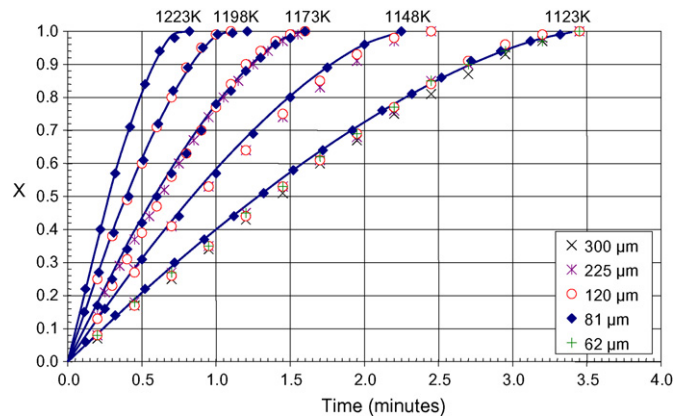


Fig. 13. Comparison of the experimental data and the results calculated with Eq. (8).

The value obtained for the apparent activation energy, corresponding to the direct chemical reaction of the thermal decomposition, was 175 kJ/mol; this is of the same order as the values proposed by other authors.<sup>22–25</sup>

### 3. Comparison of the experimental and the calculated results

Eqs. (6) and (7) yield:

$$1 - (1 - X)^{2/3} = \frac{2}{3} S_e 367 \exp\left(-\frac{175384}{RT}\right) c_B^{0-2/3} t \quad (8)$$

Using this equation it has been attempted to reproduce the results obtained in the experiments conducted under isothermal conditions. The values calculated with this equation, under the different test operating conditions with the different studied particle size fractions, have been plotted in the form *X* = *f*(*t*) (solid line), together with the experimental results in Fig. 13. The calculated values of *X* fit well with those obtained experimentally for the particle size fractions indicated in the first paragraph of Section 4.

These results indicate that Eqs. (3) or (4) appear to be sufficiently representative of the rate at which the chemical step of calcium carbonate thermal decomposition unfolds, at least in the case of calcite particles with similar physical properties to those of the particles studied, in the tested temperature range.

### 4. Conclusions

In this study a rate equation is proposed for the direct reaction in the chemical step of calcium carbonate thermal decomposition in calcite particles consisting of porous crystalline aggregates of CaCO<sub>3</sub> microcrystals smaller than 20 μm. The particles studied are of the same nature as those contained in the raw material mixtures used in industry to fabricate white-firing wall tile bodies that should decompose completely during firing in a temperature range of 850–925 °C.

In addition, an expression has been derived, based on the *Uniform Conversion Model*, which relates the calcium carbonate fractional conversion degree to the operating variables (time and



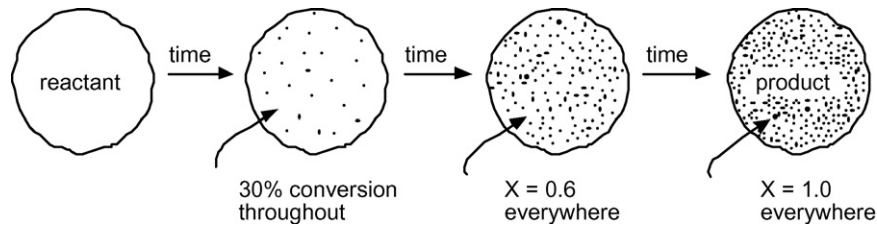


Fig. A.1. Behaviour of UCM.

temperature) and which allows the experimental results obtained under isothermal conditions to be correlated in the tested temperature range (850–950 °C), when the thermal decomposition of these calcite particles, with an average radius smaller than 120  $\mu\text{m}$ , is studied. The interpretation of the results obtained for average particle radius values larger than 120  $\mu\text{m}$  will be published in a subsequent paper.

### Acknowledgements

The authors thank the Instituto de la Mediana y Pequeña Empresa de Valencia (IMPIVA) of the Generalitat Valenciana for its financial help. They are also grateful for the support of FEDER funds from de European Unión. Project reference IMIDIC/2007/102.

### Appendix A. Application of the Uniform Conversion Model (UCM) to the process studied

The  $\text{CaCO}_3$  chemical decomposition reaction is reversible and may be expressed, using the generalised nomenclature, by the reaction scheme:



where  $\text{B} = \text{CaCO}_3$ ,  $\text{P} = \text{CaO}$ ,  $\text{Q} = \text{CO}_2$ , and  $-v_B = v_P = v_Q = 1$ . It will be assumed that all grains (microcrystals) of  $\text{B}$  ( $\text{CaCO}_3$ ) making up the particle (pellet) considered decompose progressively, crazing and cracking, giving rise to a very porous solid  $\text{P}$  ( $\text{CaO}$ ) that offers practically no resistance to diffusion through the solid (intragrain diffusion) of the gas component  $\text{Q}$  ( $\text{CO}_2$ ) resulting from calcium carbonate decomposition. So that the chemical decomposition reaction may be assumed to take place simultaneously in practically the entire mass of each microcrystal and that the gas component  $\text{Q}$  also moves very rapidly through the porous structure of each particle (crystalline aggregate) by intergrain diffusion.

In this case, the decomposition reaction may be viewed as occurring homogeneously throughout each particle to produce a gradual variation in solid reactant ( $\text{B}$ ) concentration,<sup>10,12</sup> thus allowing the *UCM* to be applied to this process. Fig. A.1 schematically illustrates the progressive changes that a calcite particle undergoes according to the *UCM*.<sup>12</sup>

On the other hand, according to this kinetic model the gaseous product concentration ( $c_Q^S$ ) is practically uniform throughout each particle, it being a little larger in the centre than at the particle–gas interface.<sup>14</sup> Fig. A.2 schematically illustrates the kinetic model considered.

In the following, the *UCM* will be applied to the process studied based on the following assumptions:

- The gas in contact with the external particle surface has a constant composition because it is continually renewed.
- The  $\text{CO}_2$  is evacuated as soon as it crosses the *particle surface/gas* interface, drawn along by the gas stream.
- The temperature is uniform throughout the very small particles (radius  $\leq 120 \mu\text{m}$ ) and remains constant during the entire thermal decomposition process.
- To simplify, the overall process rate is assumed not to be appreciably influenced by heat transmission from outside into each particle, because of the small particle size. On the other hand it is also assumed that the phenomenon of heat transmission from the gas to the surface of each particle, at the tested gas velocities, takes place at a much faster rate than the remaining physical and chemical process steps.
- The shape of the particles is spherical.
- The particles have a highly porous structure and are made up of many spherical grains (microcrystals), with a size smaller than 20  $\mu\text{m}$ , of solid reagent  $\text{B}$  (Figs. A.2 and A.3).
- The volume and internal structure of each particle are assumed not to change during the decomposition process.
- The reaction interface is the  $\text{CaCO}_3/\text{CaO}$  boundary, in each grain ( $\text{CaCO}_3$  microcrystal), and it is equal to the overall

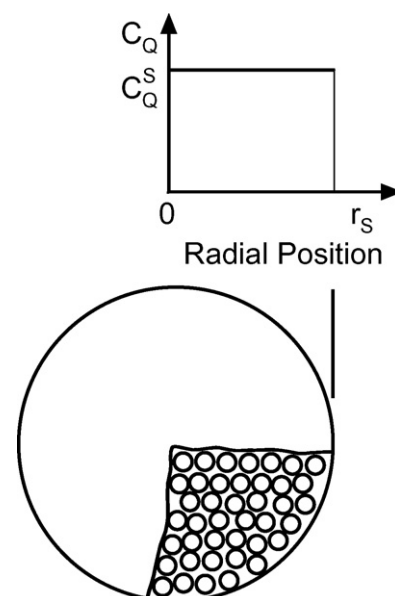


Fig. A.2. The Grainy Model for the case of a particle undergoing reaction under conditions of chemical control.



area available, outside and inside each particle, which it is assumed may be calculated from the expression:

$$S_i = S_{sp} V_{pB}^0 \quad (\text{A.2})$$

where  $S_{sp}$  is the specific surface area of the calcite particles ( $\text{m}^2/\text{m}^3$  of the total volume) and  $V_{pB}^0$  is the initial volume of each calcite particle, which is assumed not to change.

- (i) The small grains in the particle (microcrystals) craze during the decomposition process and the solid product (CaO) shell resulting is uniform (isotropic behaviour) and very porous.
- (j) The transfer of the gaseous component Q from the particle surface to the gas phase is assumed to occur very quickly, since the particles are located in a gas stream that is sufficiently rapid to allow this assumption to be made.

In this figure:

$r_s$  = initial radius of the sphere-shaped particle (m), which is assumed to remain constant.

$c_{Qi}^S$  = molar concentration of Q at the reaction interface ( $\text{kmol Q}/\text{m}^3$ ), uniformly distributed throughout the particle.

$c_{QS}^S$  = molar concentration of Q next to the particle–gas interface (solid side) ( $\text{kmol Q}/\text{m}^3$ ).

$c_{QS}^G$  = molar concentration of Q next to the particle–gas interface (gas side) ( $\text{kmol Q}/\text{m}^3$ ).

$c_Q^G$  = molar concentration of Q in the gas phase ( $\text{kmol Q}/\text{m}^3$ ).

Given the characteristics of the system (shell of CaO with relatively high porosity), the solid–gas interface is assumed to obey:  $c_{QS}^S \approx c_{QS}^G$  (see Fig. A.2).

In order to obtain a differential equation that would relate the calcite degree of conversion ( $X$ ) with reaction time ( $t$ ), in conformity with the chosen kinetic model, the mass balance was applied to a  $\text{CaCO}_3$  particle, the reactant taken as the reference component, considering each particle as an intermittent reaction system, testing different values of the partial reaction order for the direct reaction of the chemical reaction step.

The reverse reaction was considered as a first-order reaction in respect to carbon dioxide, as suggested in the literature,<sup>20</sup> even though, in the series of experiments set out in this study, it was intended to operate by making air that was practically free

of  $\text{CO}_2$  flow through the reactor. It may be noted that in a recent publication,<sup>21</sup> the first-order for the reverse reaction has been confirmed.

Several rate equations for the calcium carbonate chemical decomposition step were tested in order to choose the one that provided the best fit with the experimental results. The rate equation that led to the mathematical expression that best fitted the experimental results was

$$r = kc_B^{1/3} - k'c_{Qi}^S = k[c_B^0(1 - X)]^{1/3} - k'c_{Qi}^S \quad (\text{A.3})$$

where  $r$  is expressed in  $\text{kmol}/(\text{min m}^2)$ ,  $k$  in  $\text{kmol}^{2/3}/(\text{m min})$ , and  $k'$  in  $\text{m}/\text{min}$ . In this expression  $c_B$  and  $c_{Qi}^S$  are the molar concentration of calcium carbonate in the particle considered, and the molar concentration of carbon dioxide at the reaction interface, respectively. This equation was obtained by introducing small changes in another equation, which led to an expression  $X=f(t)$  that fitted the experimental data quite well, though not as well as when Eq. (A.3) was used.

In accordance with this equation, the reaction rate of component B, expressed in reacted  $\text{kmol}$  of B/min in the particle considered, taking into account Eq. (A.2), may be written in the form:

$$R_B = v_B S_e V_{pB}^0 [kc_B^{0/3} (1 - X)^{1/3} - k'c_{Qi}^S] \quad (\text{A.4})$$

Applying the mass balance to a particle of B gives:

$$R_B = \frac{dN_B}{dt} = V_{pB}^0 \frac{d\rho_B}{dt} \quad (\text{A.5})$$

since particle volume ( $V_{pB}^0$ ) is assumed to remain unchanged throughout the decomposition process ( $V_{pB} = V_{pB}^0$ ). On the other hand,  $\rho_B$ , the apparent molar density of the reference solid reactant, varies as the reaction advances, because the calcium carbonate decomposes progressively, so that its molar concentration or molar density in the particle considered ranges from  $\rho_B^0$  (for  $t=0$ ) to 0 (when component B has been entirely consumed).

Taking into account that the relationship between the degree of conversion ( $X$ ) and molar density of B ( $\rho_B$ ), in this case, is

$$X = \frac{N_B^0 - N_B}{N_B^0} = \frac{\rho_B^0 - \rho_B}{\rho_B^0} \quad (\text{A.6})$$

deriving with respect to  $t$  gives:

$$\frac{d\rho_B}{dt} = -\rho_B^0 \frac{dX}{dt} \quad (\text{A.7})$$

Eqs. (A.5) and (A.7) then give:

$$R_B = -V_{pB}^0 \rho_B^0 \frac{dX}{dt} \quad (\text{A.8})$$

Eqs. (A.8) and (A.4), taking into account that  $v_B = -1$ , that  $c_{Qi}^S \approx c_{QS}^S = c_{QS}^G$  (molar concentration of  $\text{CO}_2$  at the interface, gas phase side), since the chemical reaction is assumed to develop simultaneously throughout the entire mass of the particle and the intergrain diffusion step is assumed to be very rapid, allow the assumption, in the UCM, that  $c_{Qi}^S$  is practically constant throughout the particle. If, in addition, it is assumed that  $c_{QS}^G \approx c_Q^G$  ( $\text{CO}_2$  concentration in the gas phase) given that the

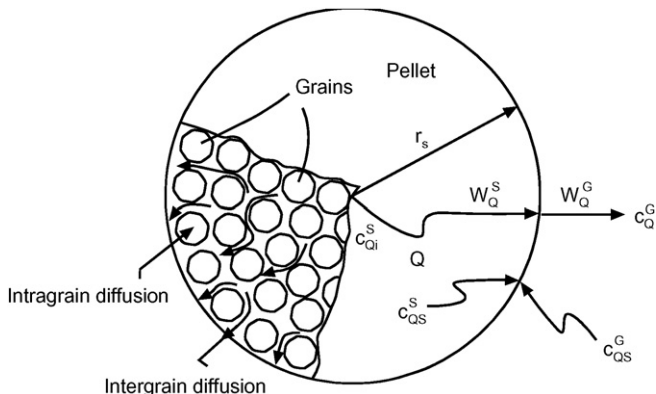


Fig. A.3. Scheme of the kinetic model considered.

transfer step of this gas from the particle–gas interface to the gas phase is developed, in this case, very rapidly, the following equation is obtained:

$$\frac{dX}{dt} = \frac{S_e}{\rho_B^0} [kc_B^{0/3} (1 - X)^{1/3} - k'c_Q^G]$$

which taking into account the equivalence between  $\rho_B^0$  and  $c_B^0$ , may be put in the form:

$$\frac{dX}{dt} = \frac{S_e}{c_B^0} [kc_B^{0/3} (1 - X)^{1/3} - k'c_Q^G] \quad (\text{A.9})$$

Considering that in all the experiments referred to in this section the molar concentration of CO<sub>2</sub> in the gas phase ( $c_Q^G$ ) was negligible, since decomposition took place in an air stream practically free of carbon dioxide, if in Eq. (A.9) one sets  $c_Q^G = 0$  and integrates between indefinite limits, the following expression is obtained:

$$1 - (1 - X)^{2/3} = \frac{2}{3} S_e k c_B^{0-2/3} t \quad (\text{A.10})$$

## References

- Smith, A. N., Investigations on the moisture expansion of porous ceramic bodies. *Trans. Br. Ceram. Soc.*, 1955, **54**(5), 300–318.
- Sánchez, E., García, J., Sanz, V. and Ochandio, E., Raw material selection criteria for the production of floor and wall tiles. *Tile Brick Int.*, 1990, **6**(4), 15–21.
- Amorós, J. L., Escardino, A., Sánchez, E. and Zaera, F., Stabilità delle dimensioni nelle piastrelle porose monocotte. *Ceram. Inf.*, 1993, **324**, 56–67.
- Sánchez, E., García-Ten, J. and Regueiro, M., Materias para la industria cerámica española. Situación actual y perspectivas. *Bol. Soc. Esp. Ceram. Vidr.*, 2006, **45**(1), 1–12.
- Beltrán, V., Sánchez, E., García-Ten, J. and Ginés, F., Materias primas empleadas en la fabricación de baldosas de pasta blanca en España. *Téch. Cerám.*, 1996, **241**, 114–128.
- Todor, D. N., *Thermal Analysis of Minerals*. Abacus Press, Tunbridge Wells, 1976.
- Adonyi, Z., Correlation between kinetic constants and parameters of differential thermogravimetry, in the decomposition of calcium carbonate. *Period. Polytech.*, 1967, **11**(3/4), 325–336.
- Beruto, D. and Searcy, A. W., Use of Langmuir method for kinetic studies of decomposition reactions: calcite CaCO<sub>3</sub>. *J. Chem. Soc. Faraday Trans.*, 1974, **70**, 2145–2153.
- Foust, A. S., Wenzel, L. A., Clump, C. W. and Andersen, L. M., *Principles of Unit Operations*. John Wiley, 1960, pp. 525–539.
- Ishida, M. and Wen, C. Y., Comparison of kinetic and diffusional models for solid–gas reactions. *AIChE J.*, 1968, **14**, 311–317.
- Doraiswamy, L. K. and Sharma, M. M., *Heterogeneous Reactions: Analysis, Examples, and Reactor Design: Volume 1: Gas–Solid and Solid–Solid Reactions*. John Wiley and Sons, New York, 1984, pp. 450–456.
- Levenspiel, O., *El Omnilibro de los Reactores Químicos*. Reverté, Barcelona, 1986, pp. 55.3–55.4.
- Sohn, H. and Szekey, J., A structural model for gas–solid reactions with a moving boundary-III. *Chem. Eng. Sci.*, 1972, **27**, 763–778.
- Szekey, J., *Gas–Solid Reactions*. Academic Press Inc., London, 1976, pp. 128–130.
- Szekey, J. and Evans, J. W., *Chem. Eng. Sci.*, 1970, **25**, 1091; Szekey, J. and Evans, J. W., *Chem. Eng. Sci.*, 1971, **26**, 1091.
- Calvelo, A. and Smith, J. M., *Proc. Chemeca*, 1970.
- Pigford, R. L. and Sliger, G., Rate of diffusion-controlled reaction between a gas and a porous solid sphere. *Ind. Eng. Chem. Proc. Des. Dev.*, 1973, **12**, 85.
- Szekey, J., Lin, C. I. and Sohn, H. Y., *Chem. Eng. Sci.*, 1973, **28**.
- Sohn, H. Y. and Szekey, J., The effect of intragrain diffusion on the reaction between a porous solid and a gas. *Chem. Eng. Sci.*, 1974, **29**, 630–634.
- Hyatt, E. P., Cutler, I. B. and Wadsworth, M. E., Calcium carbonate decomposition in carbon dioxide atmosphere. *J. Am. Ceram. Soc.*, 1958, **41**(2), 70–74.
- Escardino, A., Garcia-Ten, J. and Mestre, S., Influence of CO<sub>2</sub> content on CaCO<sub>3</sub> particle decomposition kinetics. In *Proceedings of the 10th Mediterranean Congress of Chemical Engineering*, 2005.
- Splichal, J., Skramovsky, S. and Goll, J., A stathmographic and kinetic investigation of the thermal decomposition of lime-stone. *Collect. Czechoslov. Chem. Commun.*, 1937, **9**, 302–314.
- Elder, J. P. and Reddy, V. B., The kinetics of the thermal degradation of calcium carbonate. *J. Therm. Anal.*, 1986, **31**, 395–405.
- Ninan, K. N., Krishnan, K. and Krishnamurthy, V. N., Kinetics and mechanism of thermal decomposition of in situ generated calcium carbonate. *J. Therm. Anal.*, 1991, **37**, 1533–1543.
- Rajeswara Rao, T., Kinetics of calcium carbonate decomposition. *Chem. Eng. Technol.*, 1996, **19**, 373–377.